

DEVELOPMENT OF METROLOGICAL NDE METHODS FOR MICROTURBINES CERAMIC COMPONENTS*

H.-R. Lee and W. A. Ellingson

Energy Technology Division
Argonne National Laboratory
Argonne, IL 60439

RECEIVED
MAR 07 2000
OSTI

The submitted manuscript has been created by the University of Chicago as Operator of Argonne National Laboratory, under Contract W-31-109-Eng-38 with the U.S. Department of Energy. The U.S. Government retains for itself, and others acting on its behalf, a paid-up, nonexclusive, irrevocable worldwide license in said article to reproduce, prepare derivative works, distribute copies to the public, and perform publicly and display publicly, by or on behalf of the Government.

Submitted to the 45th ASME Gas Turbine and Aeroengine Technical Congress Exposition and Users Symposium, sponsored by ASME, Munich, Germany, May 9-11, 2000

*Work supported by the U.S. Department of Energy (DOE), Office of Energy Efficiency and Renewable Energy/Advanced Turbine Systems Program, under Contract W-31-109-Eng-38.

DISCLAIMER

This report was prepared as an account of work sponsored by an agency of the United States Government. Neither the United States Government nor any agency thereof, nor any of their employees, make any warranty, express or implied, or assumes any legal liability or responsibility for the accuracy, completeness, or usefulness of any information, apparatus, product, or process disclosed, or represents that its use would not infringe privately owned rights. Reference herein to any specific commercial product, process, or service by trade name, trademark, manufacturer, or otherwise does not necessarily constitute or imply its endorsement, recommendation, or favoring by the United States Government or any agency thereof. The views and opinions of authors expressed herein do not necessarily state or reflect those of the United States Government or any agency thereof.

DISCLAIMER

Portions of this document may be illegible in electronic image products. Images are produced from the best available original document.

DEVELOPMENT OF METROLOGICAL NDE METHODS FOR MICROTURBINE CERAMIC COMPONENTS

H.-R. Lee and W. A. Ellingson
Energy Technology Division
Argonne National Laboratory
Argonne, IL 60439

Abstract

In this work, X-ray computed tomographic imaging technology with high spatial resolution has been explored for metrological applications to Si_3N_4 ceramic turbine wheels. X-ray computed tomography (XCT) data were acquired by a charge-coupled device detector coupled to an image intensifier. Cone-beam XCT reconstruction algorithms were used to allow full-volume data acquisition from the turbine wheels. Special software was developed so that edge detection and complex blade contours could be determined from the XCT data. The feasibility of using the XCT for dimensional analyses was compared with that of a coordinate-measuring machine. Details of the XCT system, data acquisition, and dimensional comparisons will be presented.

1 Introduction

Microturbine electric power generating systems using ceramic turbine wheels are estimated to have efficiencies of ~30% to >40% over similar systems that use metal wheels. However, reliable production volumes have yet to be demonstrated for the ceramic turbine wheels. Important factors in volume production are the reliability of as-produced dimensions and the detection and measurement of internal defects. Determination of the size, shape, and specific location of various aspects of a component with a complex shape can be time-consuming and thus very expensive. For components of turbine engines such as blades, vanes, or integral BLISKS, dimensions are usually verified with a coordinate-measuring machine (CMM). However, if critical internal-cooling channels or other internal shapes are complex, CMM devices cannot be used because there is no access to the area to be measured. The X-ray computed tomographic image has been used for many years in the medical and industrial communities to determine the quality of components and to provide information about processing of new materials (Mohr and Little, 1995, Illerhaus and

Thomson, 1999, and Flisch et al., 1999). More recently, because of high quality industrial X-ray computed tomography (XCT) systems, it is now possible to make detailed geometric measurements on industrial components (Yancey et al., 1995 and Little and Janning, 1998). In fact, the American Society of Mechanical Engineers has established a special committee, B-89, to address the development of standards for XCT metrology.

The objective of XCT-aided metrology (XCTAM) is to obtain geometrical information about a scanned object from a point-cloud function or an edge function of XCT reconstruction. Ideally, the XCT reconstruction process should produce clear, sharp images that correlate closely with object density. If high-quality XCT images are generated, density and wall thickness can be measured from the reconstructed images, and various edge detection algorithms can be used to determine the boundary of the object from the reconstructed images (Thirion, 1994). In reality, however, several factors, such as pixel noise of a detector, combine to degrade the reconstructed images by blurring the edge of the images and producing reconstruction artifacts. This results in the degradation of the images, and then in the distortion of the edge detection. Currently, industrial XCT systems utilize calibration procedures and image compensation algorithms to minimize image artifacts and thus enhance images to acquisition of metrological data.

This paper, which describes one application of XCTAM to determine the dimensions and shapes of Si_3N_4 turbine wheels, includes edge-detection, metrological measurements, and a comparison of XCTAM and CMM methods.

2 X-ray CT Reconstruction

In this work, the selected test specimen was an available injection-molded T-3 Si_3N_4 rotor (Fig. 1) that was developed for automotive turbocharger use.

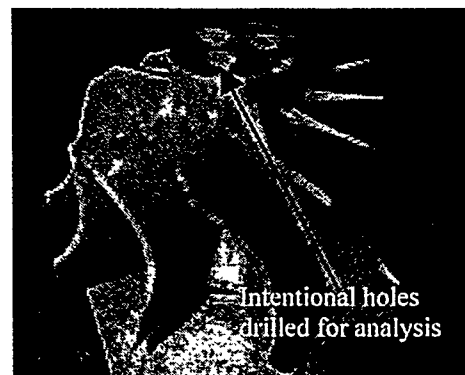


Fig. 1. Injection-molded, T-3 Si_3N_4 rotor developed for automotive turbocharger use.

(A full-size electric power microturbine wheel was not available. However, the methods and results are applicable to microturbine rotors.) XCT data were obtained with an X-320 CT scanner, which consists of a 320-kVp TFI Gemini-III X-ray source and a detector system that is an X-ray-image intensifier (XII) coupled to an ordinary 8-bit CCD camera. The X-320 scanner has a focal spot size of $\approx 300 \mu\text{m}$ and produces a maximum power of $\approx 6 \text{ kW}$. The tri-field XII has a 20-cm-diameter input screen that is coated with CsI scintillator powder, and a 2-cm-diameter output lens. The CCD camera coupled to the XII contains a 568×480 -pixel active area, with a unit-pixel size of $9 \times 9 \mu\text{m}^2$ and an 8-bit dynamic range. For this work, projection images were obtained with the X-ray source operating at 170 kVp/1.4 mA.

During the XCT scan, 360 frames of two-dimensional (2-D) projections were captured over a rotation of 360° and saved into a CT-scan file, which would be input for three-dimensional (3-D) cone-beam reconstruction (Barker et al., 1996). Figure 2a shows a typical X-ray-projection image with a size of $450 \times 180 \text{ pixels}^2$; a pixel corresponds to a physical size of $200 \times 200 \mu\text{m}^2$. Figure 2b shows a reconstructed image at the level indicated in Fig. 2a. Reconstructed-image data such as that shown in Fig. 2b were used to develop edge detection methods.

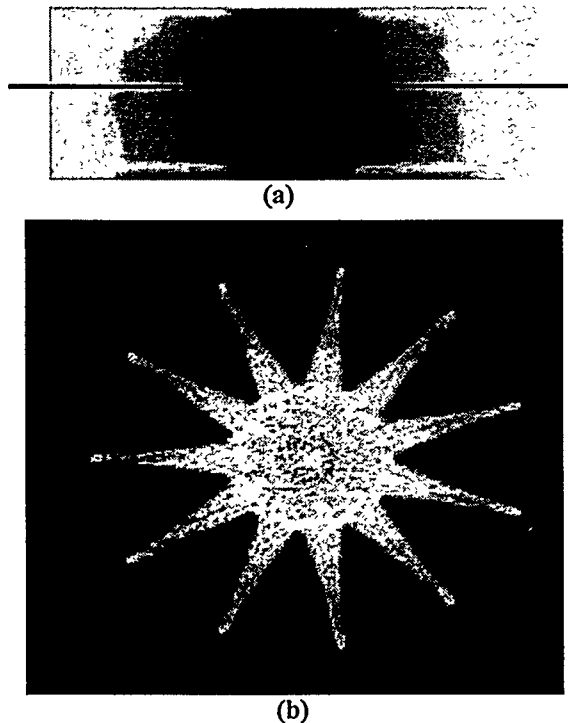


Fig. 2. X-ray images: (a) Typical X-ray projection image of part of rotor. (b) Typical XCT-reconstructed image with $170\text{-}\mu\text{m}$ -thick slice.

3 Edge Detection

The goal of edge detection from XCT images is to determine the boundary of an object. Here, our approach is to apply on the reconstructed images threshold values that are determined by image contrast. In this method, pixel intensities are determined by producing a line profile on the reconstructed images. In our work, the boundary of the object was defined with a specified reference threshold value based on 50% image contrast. The pixel deviation from the boundary was measured from pixel positions at 30 and 70% of the maximum image contrast.

Threshold-based edge detection works well when image quality is high. However, beam hardening and penetration-related artifacts, which selectively alter absolute image intensity, may contribute significant errors to edge location. In general, all artifacts increase with object size so the magnitude of edge errors increases with part size. In this work, the image-analysis codes were locally written in LabView user interface software. Assuming that the core body of the rotor has a circular symmetry, as shown in Fig. 3, we obtained an intensity profile along a circular arc with a radius of 100 pixels, which is the distance from the center of the core. The edge profiles were obtained on eight slices, with a five-slice interval for estimating an average threshold value.

As shown in Fig. 4a, the image of the object edge was extracted from the original reconstructed image shown in Fig. 2b. Figure 4b, which is an image of the original reconstruction superimposed on the edge image, shows the accuracy of the edge detecting method previously mentioned. Sequential series of the edge images were merged along the rotational axis, allowing construction of a point-cloud function, which is a 3-D edge image of the object and is used for metrological analysis of the object.

4 Metrology

Rotors, in general, have symmetrical core bodies and identical blades that are evenly spaced around the core. This arrangement leads consideration of the shape and position of blades for metrological analysis. Special software was developed locally to determine the complex blade contours from the XCT-reconstruction data. From the reconstruction data, the center of the rotor was determined and one of blade was selected as a reference to develop the calculated/interpolated contour of each blade tip. The contours were expressed in terms of radius and angle, according to Eqs. 1 and 2

$$R(z) = a + bz + cz^2 + dz^3 \quad (1)$$

$$\theta(z) = e + fz + gz^2 + hz^3 + \theta_0, \quad (2)$$

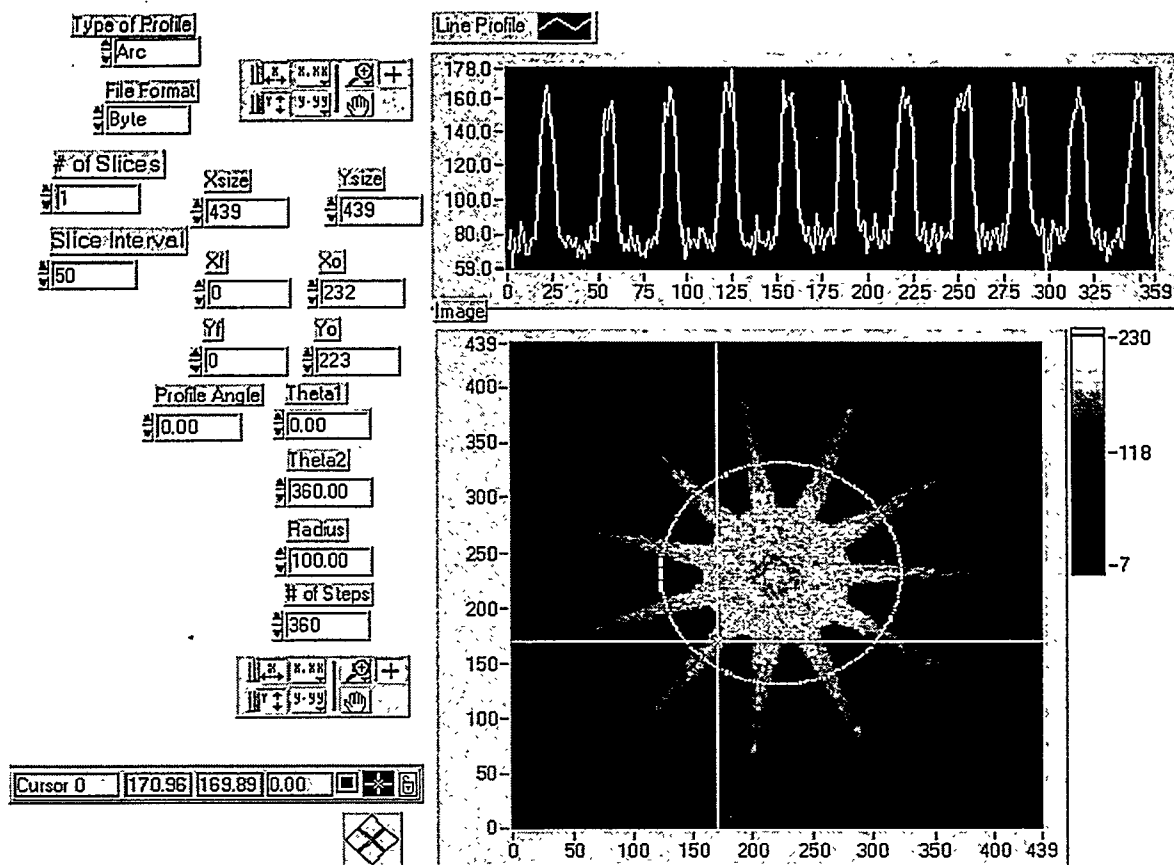


Fig. 3. Screen-captured image of LabView code for intensity profile.

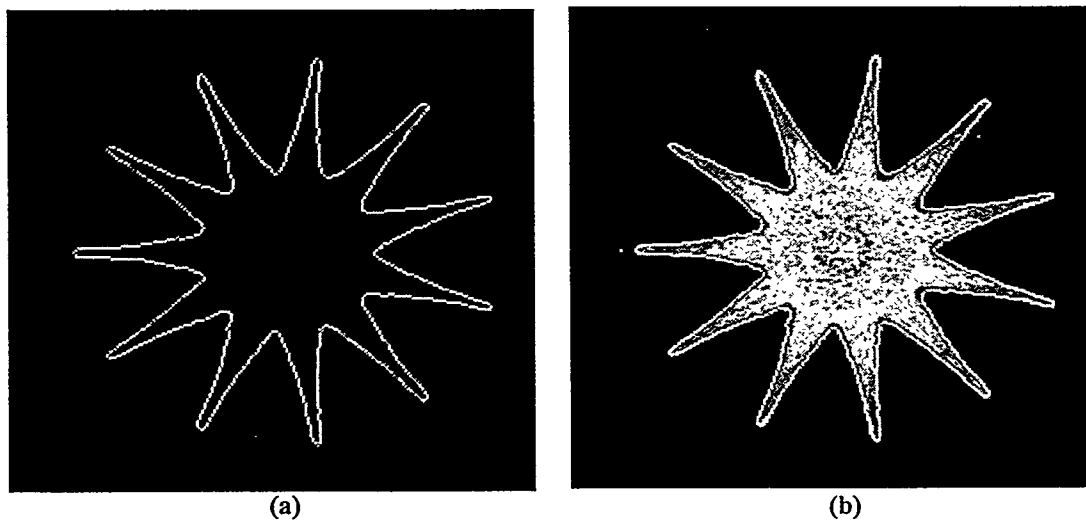
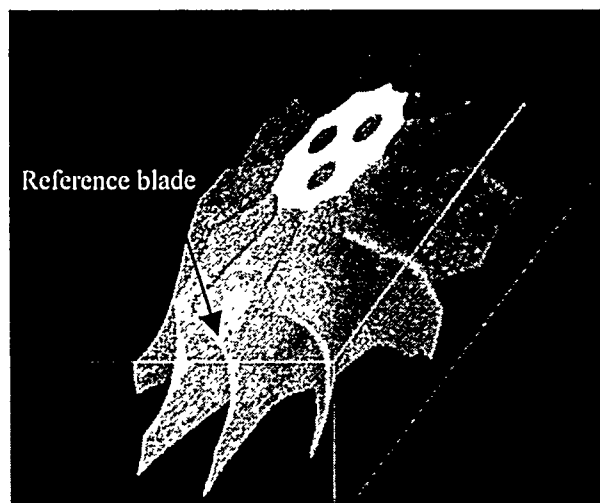


Fig. 4. Accuracy of edge detecting method: (a) Edge image of reconstructed image shown in Fig. 2b. (b) Image of reconstructed image superimposed on edge image.

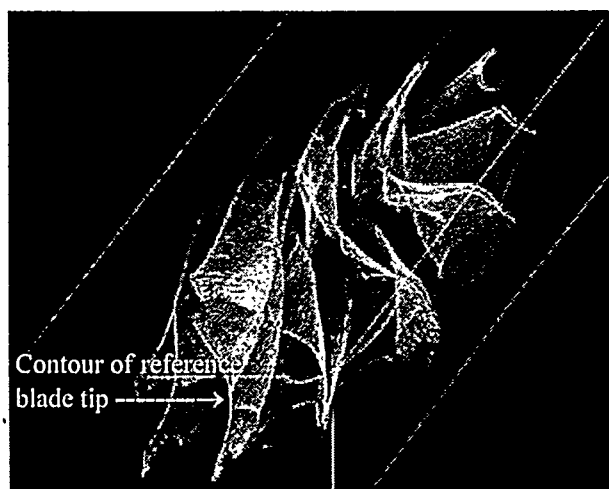
which are third-order polynomials of the z (i.e., vertical) position along the axis of rotation, where θ_0 represents the angle of shift for each blade from the reference blade. Four slices of the reconstructions

were selected to develop the polynomial functions for the contour of the reference blade. Based on these polynomials, the contours of all the blades were developed by simply adding a shift in angle.

Figure 5 shows a surface-rendered image of the 3-D reconstruction of the rotor and a point-cloud function of the rotor; the latter includes the contours of the blades in 3-D space. The contours were



(a)



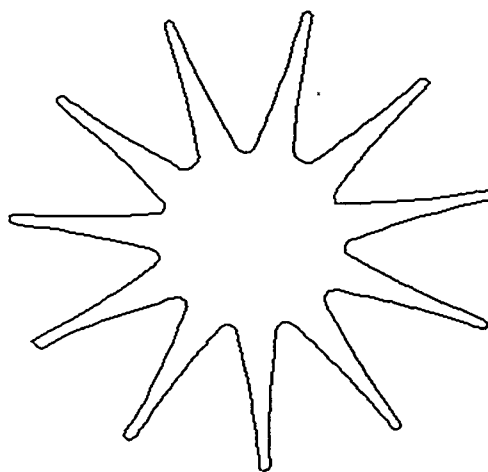
(b)

Fig. 5. Surface renderings generated from edge-detected files. (a) Surface rendering developed from reconstruction data. (b) Point-cloud function with blade tip contours.

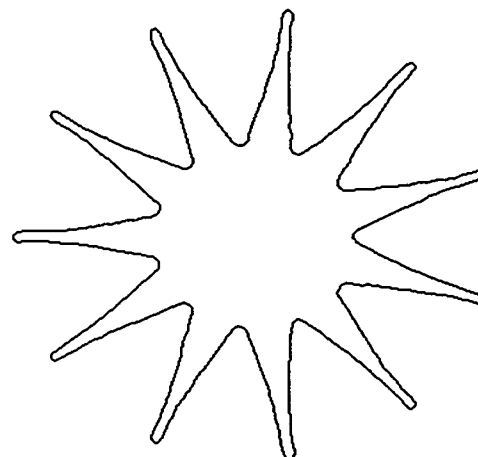
interpolated from the polynomials and inserted into the point-cloud function. By doing this, we can obtain metrological information about the rotor, i.e., the separation, position of blades, etc.. As shown in Fig. 5b, the contour of the reference blade is well matched with the shape of the blade, but the other contour positions shifts a little off the tip of the blades. With the method we have described to this point, manufacturers may be able to examine and verify production of rotors.

5 Comparison of XCTAM and CMM Techniques

To compare the XCTAM with the CMM method, we used the Argonne National Laboratory CMM machine, which is a Brown & Sharpe, Model EXCEL 7-10-7. Figure 6 shows the edge-detection images generated by both methods. (However, the edge images could not be superimposed on each other for comparison because they were developed by different software with different scales and orientations.) The CMM method generated one two-2-D edge image of the rotor after a 4-hour developing procedure because the turbine was complex. The tolerance of this measurement was ± 0.5 mm in the vertical direction and ± 0.025 mm in the horizontal direction. On the other hand, the XCTAM shows a



(a)



(b)

Fig. 6. Edge detection images of Fig. 2b generated by (a) CMM, and (b) XCTAM.

tolerance of ± 0.2 -mm in both directions. This tolerance corresponds to the spatial resolution of the reconstructed images and provides the entire 3-D point-cloud function from the 3-D reconstructed image in <1 minute

6 Summary

An initial comparison has been made between results obtained from a CMM machine and those obtained from one approach to XCTAM when used to acquire geometrical information about a ceramic microturbine. An XCT scan was performed on an injection-molded, T-3 Si_3N_4 rotor by utilizing an X-320 CT scanner. With the CT-scan data, we developed a 3-D-reconstructed image with a spatial resolution of 200 μm . From this 3-D image, we generated a point-cloud function by applying a threshold technique. The boundary of the object was defined with a specified reference threshold value based on 50% image contrast. The point-cloud function, which is an edge function of the XCT reconstruction was used to obtain geometrical information about the scanned object. The blade-tip contour was determined from the point-cloud function, in which the XCTAM shows ± 200 - μm tolerance and a fast dimensional analysis within <1 min. In the future, we must verify the accuracy of the XCTAM, which depends on various factors, such as the number of projections, which is determined by the complexity and size of an object, and the threshold values that must be applied to develop an edge detection image.

Acknowledgment

Work supported by the U.S. Department of Energy (DOE), Office of Energy Efficiency and Renewable Energy/Advanced Turbine Systems Program, under Contract W-31-109-Eng-38.

References

Barker, M. D., Subramonian, R., and Jaffrey, S., 1996, "Three-Dimensional Computed Tomography Using Parallel Processing," Proceedings of the ASNT Industrial Computed Tomography topical conference, May 13-15, Huntsville, Alabama.

Flisch, A., et al, 1999, "Industrial Computed Tomography in Reverse Engineering Application," in proceedings of Computerized Tomography for Industrial Application and Image Processing in Radiology, Berlin, March 15-19, pp. 45-53.

Illerhaus, B. and Thompson, J. L., 1999, "Calculating CT Data from Matched Geometries," in proceedings of Computerized Tomography for Industrial

Applications and Image Processing in Radiology, Berlin, March 15-17, pp. 180-191.

Little, F. H. and Janning, J. C., 1998, "Computed Tomography Metrology," U.S. Patent No. 5,848,115 issued Dec. 8, 1998.

Mohr, G. A. and Little, F., 1995 "Effective 3D Geometry Extraction and Reverse CAD Modeling," Review of Progress in Quantitative Nondestructive Evaluation, Vol. 14, ed. by D. O. Thompson and D. E. Chimenti, Plenum Press, New York, pp. 651-656.

Thirion, J. P., 1994, "Direct Extraction of Boundaries from Computed Tomography Scan," IEEE Trans. Med. Imag., Vol. 13, June 1994, pp. 311-322.

Yancey, R. N., Stanley, J. H., Eliassen, D. S., Dzigan, R., Jacobs, P., Veerabadran, T., 1995, "Integration of Reverse Engineering, Solidification Modeling, and Rapid Prototyping Technologies for the Production of Net-Shape Investment Cast Tooling," Proceedings of the 43rd Annual Technical Meeting of the Investment Casting Institute, Dallas, TX.